Highly photosensitive polymethyl methacrylate microstructured polymer optical fiber with doped core

D. Sáez-Rodríguez,[1,*] K. Nielsen,[2] H. K. Rasmussen,[3] O. Bang,[2] and D. J. Webb[1]

[1]*Aston Institute of Photonic Technologies, Aston University, Birmingham, UK*

[2]*DTU Fotonik, Department of Photonics Engineering, Technical University of Denmark, DK-2800 Kgs. Lyngby, Denmark*

[3]*Department of Mechanical Engineering, Technical University of Denmark, DK-2800 Kgs. Lyngby, Denmark*

*Corresponding author: d.saez-rodriguez@aston.ac.uk

In this Letter, we report the fabrication of a highly photosensitive, microstructured polymer optical fiber using benzyl dimethyl ketal as a dopant, as well as the inscription of a fiber Bragg grating in the fiber. A refractive index change in the core of at least 3.2×10^{-4} has been achieved, providing a grating with a strong transmission rejection of −23 dB with an inscription time of only 13 min. The fabrication method has a big advantage compared to doping step index fiber since it enables doping of the fiber without using extra dopants to compensate for the index reduction in the core introduced by the photosensitive agent.   © 2013 Optical Society of America

OCIS codes: (050.2770) Gratings; (060.2310) Fiber optics; (050.5298) Photonic crystals; (060.3738) Fiber Bragg gratings, photosensitivity; (060.4005) Microstructured fibers; (060.5295) Photonic crystal fibers.

http://dx.doi.org/10.1364/OL.38.003769

Since Hill demonstrated the possibility of inscribing fiber Bragg gratings (FBGs) in silica-based optical fibers (SOFs) [1], huge efforts have been made to improve the core photosensitivity [2] in order to enhance the efficiency of grating fabrication. These improvements in silica fiber have enabled a wide range of applications, especially in the fields of sensors and telecommunication [2].

Nowadays, polymer optical fiber (POF) Bragg gratings are at the same evolution point as SOFs were 20 years ago and have similar drawbacks, such as the lack of photosensitivity [3]. However, in regards to their use as sensors, POF Bragg gratings have demonstrated some advantages over silica fibers. For example, the small Young's modulus together with the low stiffness of polymethyl methacrylate (PMMA) enables sensing of compliant structures [4] and the development of sensitive fiber optical accelerometers [5], and PMMA-based POFs have an elastic limit around 10% as compared to 1% for silica [6]. Moreover, the strain sensitivity of PMMA-based POF Bragg gratings has been reported to be 22% greater than the strain sensitivity of SOF Bragg gratings, while the temperature sensitivity is three times greater than that of the SOF Bragg grating [7,8].

The photosensitivity of POFs, which is an important property for the development of good FBG sensors, can involve several mechanisms, such as photolysis [9], photopolymerization [10], photoisomerization [11] or photo-crosslinking [12]. The first evidence of PMMA photosensitivity was reported by Tomlinson *et al.*, who demonstrated the photosensitivity of undoped PMMA films when they were prepared under special conditions and irradiated by ultraviolet (UV) light [13]. Tomlinson *et al.* verified that the density of the irradiated areas increased and with it the refractive index; they attributed this density change to the photo-crosslinking mechanism. However, later, Bowden *et al.* related the process to photopolymerization [14]. Taking advantage of the inherent PMMA photosensitivity, FBGs were inscribed in PMMA microstructured polymer optical fiber (mPOF) [15,16].

Later Topas (www.topas.com) was also shown to be photosensitive and FBGs were inscribed into Topas mPOFs [17], which are humidity insensitive [18].

The photosensitivity of pure PMMA is quite low and furthermore varies along the fiber length [19]; as a consequence, some authors have worked to manufacture doped-core POF to improve its performance. First, Peng *et al.* doped the core of a step index PMMA fiber with an organic dye, demonstrating the first recorded grating in a polymer fiber [20]. Later, Peng *et al.* doped the core of a POF using ethyl and benzyl methacrylate with a low concentration of both initiator and chain transfer agent in order to improve the photosensitivity [21]. This allowed for the inscription of FBGs as strong as −28 dB [22]; however, the inscription time was very long: 85 min. Later, Tam *et al.* doped the core of a POF with a photoisomer which, when illuminated under specific UV radiation, changes from the trans-structure to the cis-structure, providing in this case a negative index change [11]. In this way, a −10 dB Bragg grating was obtained in 10 min.

Recently, Peng *et al.* doped the core of a POF using a photoinitiator called benzyl dimethyl ketal (BDK) [7]. When the fiber is illuminated by the appropriate wavelength, the photopolymerization process starts in the core and leads to a positive index change. For this fiber, an index change of 4.5×10^{-5} was reported for a dopant concentration of 10%. This result was far below that reported in BDK-doped PMMA films with the same dopant concentration, which displayed an index change of 2.4×10^{-3} [23]. The doping methods used by Peng and Tam involve the use of extra dopants in the core to compensate for the reduction in index produced by adding the photosensitizer. The use of extra dopants limited the quantity of photosensitizer (photoinitiators, photoisomers, etc.) in the core.

In this Letter, we report the fabrication of a BDK-doped mPOF and the inscription of an FBG with an index change of at least 3.2×10^{-4}, which is the strongest index change reported in a polymer fiber. The use of an mPOF offers a key advantage in that, unlike with step index fibers, no additional dopants or copolymers are required to control the core index. This is possible due to the photonic crystal effect where the hole structure reduces the average index of the cladding allowing guiding in the core [24] in a similar way to waveguiding in the step index fiber. If the ratio of hole size to pitch is big enough, the guiding mechanism can be as a result of the presence of photonic band gaps [25], in which case light can be confined the core even if its effective index is smaller than the cladding. Therefore, the maximum amount of dopant in the core will depend on the size of the holes in the cladding.

The fabrication of the doped mPOF was made in three steps. First, a commercial PMMA rod of 60 mm diameter was pulled on the drawing tower to produce a structure-less solid cane with 5.23 mm diameter. This rod was then introduced into a solution of methanol and BDK in the proportion of $3:1$ by weight. The methanol (from Merck) had 99.9% purity. Methanol acts as a diffusion enhancer inside the PMMA, as it effectively increases the mobility and therefore the deposition of BDK in the PMMA [26]. After nine days at room temperature, the rod was extracted from the solution and immediately turned from transparent to a white color. This revealed that the highly volatile methanol had started to evaporate, leaving the BDK behind. After 10 min, the rod became transparent again. Figures 1(a) and 1(b) show the white rod and the transparent rod. Figure 1(c) shows an optical microscope image of the transverse structure of the rod four days after it was extracted from the solution. Here, it can be seen that the methanol–BDK solution has diffused into the rod. The two concentric color circles show that the rod was not in the solution for sufficient time to allow the BDK to reach the center.
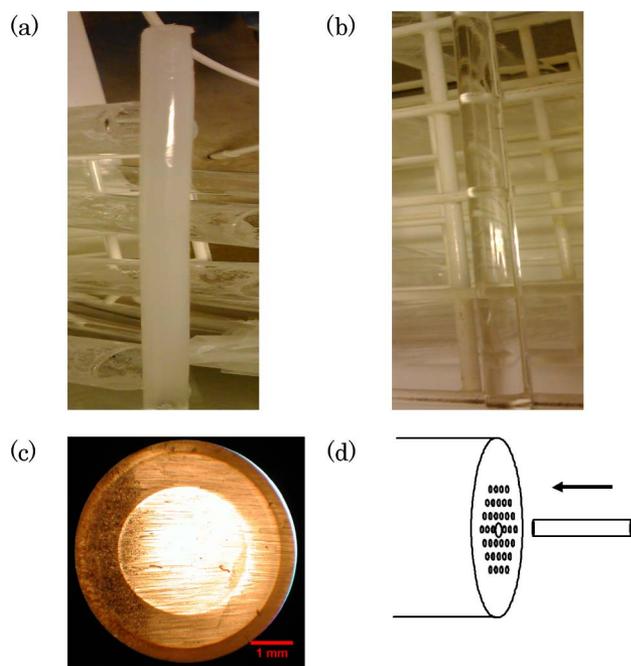
In the second step, the doped rod was introduced into the center hole of a preform, which had a three-ring hexagonal cladding structure as shown in Fig. 1(d). The diameter of the holes in the cladding was $d = 2.5$ mm and the pitch was $\Lambda = 6.2$ mm. The central hole had a diameter of 5.3 mm. The doped rod was smaller than the core (we define the core as $2\Lambda - d = 9.9$ mm) to reduce the diffusion of the dopant to the cladding during drawing. This preform was then drawn to canes of diameter 5.2 mm.

Finally, in the third step, the fiber was fabricated. The mPOF cane with a doped core made in the previous step was sleeved with three PMMA tubes with outer/inner diameters of 10/7, 15/11, and 20/16 mm, respectively, forming a new preform, which was then drawn to fiber. In Figs. 2(a) and 2(b), we show optical microscope images of the core region of the doped cane and of the final mPOF, respectively. In the center of both images, it is possible to distinguish the dopant. The average pitch and hole diameter in the fiber are 3.7 and 1.74 μm, respectively, and the external diameter is 130 μm. This results in a relative hole diameter of $d/\Lambda = 0.47$.

A CW He–Cd laser with an output power of 30 mW at 325 nm was used to inscribe an FBG in the doped mPOF. The inscription was carried out using a mirror mounted on a motorized translation stage to scan a beam of 1.2 mm diameter focused with a cylindrical lens (focal length approximately 6 cm) along the fiber through a phase mask of pitch 557.5 nm. The final grating length was 3.8 mm. Figure 3(a) shows the growth of the transmission spectrum during the first 13 min, measured by terminating both ends of the mPOF with FC/PC connectors [27]. The resonance wavelength was 826.95 nm and the notch viewed in transmission had a depth of –23 dB and width of 0.3 nm at –10 dB.

The grating growth after 13 min is shown in Fig. 3(b); during this period, it was not possible to measure a depth greater than –23 dB because of the power of the light source and the fiber losses. However, over this time we observed an increase of the width, meaning that the grating continues to increase in strength. After 30 min of inscription, the width had increased to 0.55 nm at –10 dB.

From Fig. 3, additional information can be extracted related to the index modulation. The resonance wavelength has a red-shift during the inscription revealing that the refractive index change is positive, as is expected

(a) (b) (c) (d)

Fig. 1. Doped rod (a) 10 s and (b) 10 min after extraction from the solution. (c) Transverse structure of doped rod. (d) Microstructured preform with a larger central hole for the doped rod.

(a) (b)
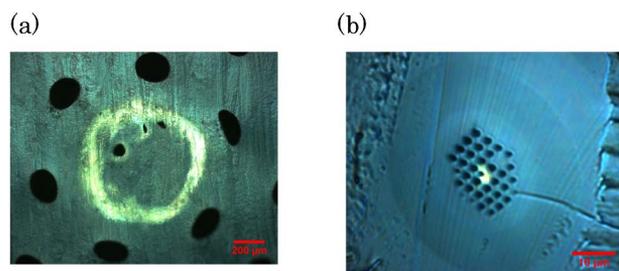
Fig. 2. In both images, the bright part is the doped region. (a) Doped cane. (b) Doped fiber.

(a)

(b)
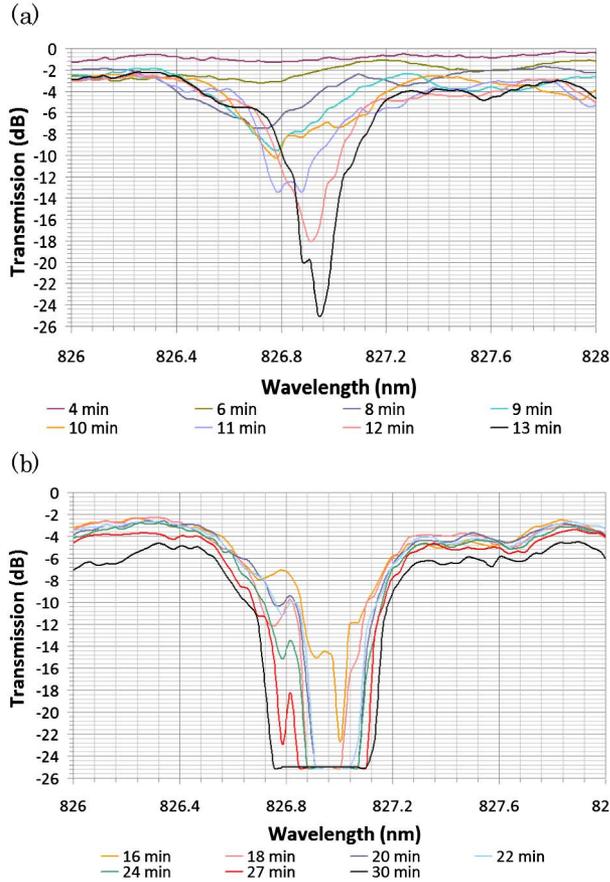
Fig. 3. Growth spectrum FBG. (a) First 13 min of inscription. (b) Inscription from 16 to 30 min.

Table 1. Time, Grating Length, and Coupling Coefficient for Every Trace of Fig. 3(a)

Time (min)	Length (cm)	K (m^{-1})
4	0.48	1164
6	0.72	1253
8	0.96	1466
9	1.08	1632
10	1.2	1534
11	1.32	1613
12	1.44	1923
13	1.56	2289
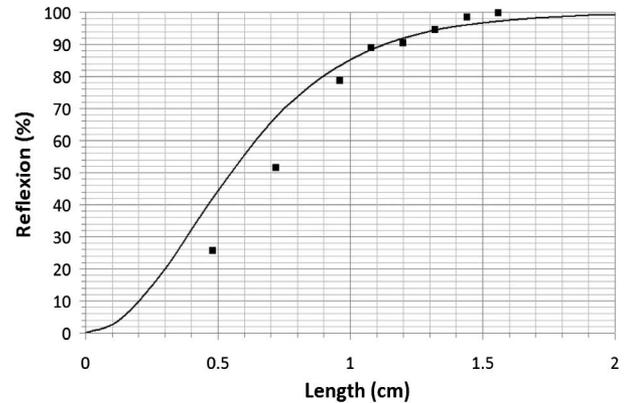
Fig. 4. Reflection against grating length. The solid line is the theory and dots the experimental results.

from a photopolymerization mechanism. In addition, the refractive index modulation amplitude of the grating region can be estimated from Fig. 3(a) to be at least 3.2×10^{-4} by the following equations [2]:

$$R = \tanh^2(K \cdot L), K = \frac{\pi \cdot \Delta n \cdot \eta}{\lambda},$$

where R is the reflectivity of the grating, L is the length of the grating after 13 min recording time, K is the coupling coefficient, Δn is the index modulation, and η represents the fraction of the integrated fundamental-mode intensity contained in the core. In the calculation, it has been assumed that $\eta = 1$ and the effective length of the grating is determined by the 1.2 mm beam diameter added to the length scanned by the beam in 13 min (1.56 mm), giving a total of 2.76 mm.

In Table 1, we have listed the coupling coefficient of each spectrum in Fig. 3(a). The coupling coefficient tends to increase during inscription because, although we are scanning the beam, the beam width is a significant fraction of the total grating length. Fluctuations in the coupling coefficient may be caused by a nonuniform dopant distribution along the fiber. In Fig. 4, a plot has been made of both theoretical and experimental reflectivity against fiber length [the experimental dots correspond to the spectra in Fig. 3(a)]. In the theoretical curve, the coupling coefficient used is 1609 m⁻¹, which corresponds to the average coupling coefficient in the experimental results. It can be seen that the experimental dots and theoretical curve fit reasonably well.

In conclusion, we have described the fabrication process of a photosensitive PMMA-based mPOF doped with BDK, and an FBG has been inscribed in the fiber displaying an index change in the core of at least 3.2×10^{-4}. This fabrication method, besides improving on the photosensitivity of previously published BDK-doped fibers, allows the doping of the fiber in a more straightforward way compared to step index POF, since it is not necessary to use extra dopants such as ethyl methacrylate in the core to compensate for the reduction of the refractive index as a consequence of the addition of the BDK dopant.

References
1. K. O. Hill, Y. Fujii, D. C. Johnson, and B. S. Kawasaki, Appl. Phys. Lett. **32**, 647 (1978).
2. A. Othonos and K. Kalli, *Fiber Bragg Grating: Fundamentals and Applications in Telecommunications and Sensing* (Artech, 1999).
3. M. C. J. Large, L. Poladian, J. W. Barton, and M. A. V. Eijkelenborg, *Microstructured Polymer Optical Fibres* (Springer Science and Business Media, 2008).
4. S. Kiesel, P. van Vickle, K. Peters, O. Abdi, T. Hassan, and M. Kowalsky, Proc. SPIE **6174**, 617435 (2006).
5. A. Stefani, S. Andresen, W. Yuan, N. Herholdt-Rasmussen, and O. Bang, IEEE Photon. Technol. Lett. **24**, 763 (2012).

6. M. C. J. Large, J. Moran, and L. Ye, Meas. Sci. Technol. **20** 034014 (2009).

7. C. Zhang, W. Zhang, D. J. Webb, and G.-D. Peng, Electron. Lett. **46**, 643 (2010).

8. H. Y. Liu, H. B. Liu, and G.-D. Peng, Opt. Commun. **251**, 37 (2005).

9. C. Wochnowski, S. Metev, and G. Sepold, Appl. Surf. Sci. **154**, 706 (2000).

10. Y. Luo, Q. Zhang, H. Liu, and G.-D. Peng, Opt. Lett. **35**, 751 (2010).

11. J.-M. Yu, X.-M. Tao, and H.-W. Tam, Opt. Lett. **29**, 156 (2004).

12. G. Oster, Polym. Lett. **2**, 1181 (1964).

13. W. J. Tomlinson, I. P. Kaminow, E. A. Chandross, R. L. Fork, and W. T. Silfvast, Appl. Phys. Lett. **16**, 486 (1970).

14. M. J. Bowden, E. A. Chandross, and I. P. Kaminow, Appl. Opt. Technol. **13**, 112 (1974).

15. I. P. Kaminow, H. P. Weber, and E. A. Chandross, Appl. Phys. Lett. **18**, 497 (1971).

16. H. Dobb, D. J. Webb, K. Kalli, A. Argyros, M. C. J. Large, and M. A. V. Eijkelenborg, Opt. Lett. **30**, 3296 (2005).

17. I. P. Johnson, W. Yuan, A. Stefani, K. Nielsen, H. K. Rasmussen, L. Khan, D. J. Webb, K. Kalli, and O. Bang, Electron. Lett. **47**, 271 (2011).

18. W. Yuan, L. Khan, D. J. Webb, K. Kalli, H. K. Rasmussen, A. Stefani, and O. Bang, Opt. Express **19**, 19731 (2011).

19. G. Harbach, "Fiber Bragg gratings in polymer optical fibers," M.S. thesis (Ecole Polytechnique Federale De Lausanne, 2008).

20. G. D. Peng, Z. Xiong, and P. L. Chu, Opt. Fiber Technol. **5**, 242 (1999).

21. Z. Xiong, G. D. Peng, B. Wu, and P. L. Chu, IEEE Photon. Technol. Lett. **11**, 352 (1999).

22. H. Y. Liu, G. D. Peng, and P. L. Chu, Opt. Lett. **14**, 935 (2002).

23. H. Franke, Appl. Opt. **23**, 2729 (1984).

24. T. A. Birks, J. C. Knight, and P. St. J. Russell, Opt. Lett. **22**, 961 (1997).

25. J. C. Knight, J. Broeng, T. A. Birks, and P. St. J. Russell, Science **282**, 1476 (1998).

26. M. C. J. Large, S. Ponrathnam, A. Argyros, N. S. Pujari, and F. Cox, Opt. Express **12**, 1966 (2004).

27. A. Abang and D. J. Webb, Opt. Eng. **51**, 080503 (2012).